Transformer-Based Classification of Parkinson's Disease from EEG Using BIDS-Formatted OpenNeuro Datasets

Raven Lee*[1], Caleb Cooper*[2], Manliang Feng[3], Jinghe Mao[4]

[1]Department of Mathematics, Tougaloo College, Tougaloo, MS, USA

[2]Department of Atmospheric Sciences, Howard University, Washington, D.C., USA

[3]Department of Chemistry, Tougaloo College, Tougaloo, MS, USA

[4]Department of Biology, Tougaloo College, Tougaloo, MS, USA

rlee@student.tougaloo.edu, caleb.cooper@bison.howard.edu, mfeng@tougaloo.edu, jmao@tougaloo.edu

Abstract

Artificial intelligence systems that support rapid and reliable decision-making under time-sensitive constraints must interpret high-dimensional sensory inputs while remaining robust to variability and noise. Electroencephalography (EEG) exemplifies such a sensing modality due to its non-stationarity, subject variability, and sensitivity to recording conditions.

This study evaluates a Transformer-based framework for multi-class classification of Parkinson's disease medication state (PD-ON, PD-OFF) and healthy controls using structured spectral and entropy-based EEG features. Rather than proposing an end-to-end raw-signal model, we assess whether attention-based sequence modeling offers advantages over classical classifiers when operating on physiologically interpretable representations. Three heterogeneous BIDS-formatted OpenNeuro datasets (PD1: n = 31; PD2: n = 50; PD3: n = 56) were evaluated using subject-wise grouped cross-validation to prevent participant-level data leakage.

The Transformer achieved near-ceiling F1-scores on relatively homogeneous datasets (PD1: 99.33%; PD3: 98.35%) and competitive performance on the more heterogeneous PD2 dataset (88.36%), underscoring the impact of sensing variability on robustness. Attention analysis indicates adaptive weighting of informative temporal–spectral features.

These findings provide a systematic empirical evaluation of attention-based sequence modeling under heterogeneous sensing conditions.

Code — https://github.com/relee2022/EEG-PD-Classification

Datasets — https://openneuro.org/datasets/ds002778/versions/1.0.2; https://openneuro.org/datasets/ds003490/versions/1.1.0; https://nemar.org/dataexplorer/detail?dataset_id=ds003506

* These authors contributed equally to this work.

1 Introduction

AI systems designed for time-sensitive autonomous operation increasingly face the challenge of making reliable decisions in complex sensory environments under operational constraints. Whether applied in defense, medicine, robotics, or human–machine teaming, these systems must process high-bandwidth data streams, adapt to uncertainty, and generate rapid, context-appropriate outputs. EEG signals, noninvasive recordings of cortical electrical activity, are particularly difficult to interpret due to their noise, variability, and rapid temporal fluctuations (Delorme, Sejnowski, and Makeig 2007; Jung et al. 2000). Developing AI models capable of extracting stable and interpretable features from EEG under such variability provides a controlled yet challenging testbed for studying robust sensing and sequential decision frameworks.

Parkinson's disease (PD), a progressive neurodegenerative disorder affecting millions worldwide, presents a compelling testbed for such approaches (Tysnes and Storstein 2017; Tarakad and Jankovic 2017). PD is associated with alterations in neural oscillations, particularly within beta-band activity, which can be captured through EEG (Brittain and Brown 2014; Little and Brown 2014; Holt et al. 2019). Traditional EEG analysis methods are time-consuming, sensitive to human subjectivity, and limited in their suitability for real-time diagnostic contexts. As a result, recent work has turned toward machine learning techniques for automated PD detection (Abdulhamit Subasi and Gursoy 2010;

Betrouni et al. 2019; Geraedts et al. 2021; Kurbatskaya et al. 2023).

In this work, EEG-based Parkinson's disease classification is formulated as a sequential decision modeling problem under sensing uncertainty rather than a static pattern recognition task. The proposed system processes segmented neural signals, extracts informative spectral and entropy-based features, and produces data-driven classifications. All evaluations are conducted offline; references to time-sensitive processing are conceptual and reflect the sequential structure of the data rather than real-time clinical deployment. A key requirement for such models is the ability to generalize across subjects and heterogeneous recording conditions, a challenge well documented in EEG research (He and Wu 2020; Zhang et al. 2023). Transformer architectures, originally developed for natural language processing and increasingly adopted for physiological signal analysis, are well suited to this setting. Through their self-attention mechanism, Transformers dynamically weight relevant neural features, allowing the model to emphasize task-critical information while suppressing noise.

Importantly, this study does not introduce a novel Transformer architecture. Instead, it provides a systematic empirical evaluation of attention-based sequence modeling applied to standardized, physiologically interpretable EEG features across multiple heterogeneous datasets.

Our study evaluates the performance, generalizability, and interpretability of a Transformer model trained to detect PD from EEG across three BIDS-formatted datasets. By benchmarking against classical ML models and examining attention patterns, we demonstrate how Transformers support accurate, fast, and explainable decision pipelines applicable to both clinical neurodiagnostics and broader autonomous system design.

2 Related Work

2.1 EEG-Based Parkinson's Disease Analysis

Prior neurophysiological studies have identified abnormal beta-band activity, reduced signal complexity, and disrupted cortical synchronization in Parkinson's disease (PD), supporting the use of EEG as a noninvasive diagnostic tool (Brittain and Brown 2014; Little and Brown 2014; Holt et al. 2019). Early EEG-based PD classification relied on handcrafted spectral and statistical features combined with classical machine learning methods, demonstrating that EEG contains disease-relevant information (Subasi and Gursoy 2010). Subsequent studies extended these approaches to clinical screening and cognitive profiling but reported limited generalizability due to EEG non- stationarity, inter-subject variability, and sensitivity to recording conditions and medication state (Betrouni et al. 2019; Geraedts et al. 2021; Kurbatskaya et al. 2023; Zhang et al. 2023). These findings underscore that within-dataset performance may not directly translate to cross-condition robustness, motivating multi-dataset evaluation frameworks.]

2.2 Attention-Based Models and Interpretability

To reduce dependence on manual feature engineering, recent work has explored deep learning approaches for EEG analysis. While convolutional and recurrent models capture local temporal structure, they often struggle with long-range dependencies and cross-subject generalization (He and Wu 2020). Transformer architectures address these limitations through self-attention mechanisms that dynamically prioritize informative temporal segments. In contrast to end-to-end raw-signal modeling approaches, the present study evaluates Transformers operating on structured spectral and entropy-based features, enabling interpretability while isolating modeling capacity from feature extraction.

2.3 Broader Decision-Making Context

EEG-based PD classification exemplifies a broader class of decision-making problems involving high-dimensional, noisy sensory inputs under time constraints. Attention-based architectures offer a general framework for adaptive information prioritization. Rather than claiming direct real-time autonomy deployment, we frame EEG classification as a structured sensing problem that reflects key properties of autonomous perception pipelines: noise, heterogeneity, and temporal dependency.

3 Experimental Procedure

3.1 Participants & Data Acquisition

This study utilizes three publicly available EEG datasets from OpenNeuro: PD1 (ds002778) acquired at the University of California, San Diego; PD2 (ds003490) from the Cognitive Rhythms and Computation Laboratory at the University of New Mexico; and PD3 (ds003506), also from the Cognitive Rhythms and Computation Laboratory at the University of New Mexico. Each dataset includes EEG recordings from individuals diagnosed with Parkinson's disease (PD) and healthy control (CTL) participants and is organized according to the Brain Imaging Data Structure (BIDS) standard, enabling consistent and reproducible data access and preprocessing. All datasets contain recordings from three experimental conditions: Parkinson's disease on medication (PD-ON), Parkinson's disease off medication (PD-OFF), and healthy controls (CTL). Participant ages across datasets range from 47 to 84 years old.

PD1 consisted of 31 participants (15 PD, 16 CTL) who completed a 2-minute eyes-closed resting-state EEG task. PD2 included 50 participants (25 PD, 25 CTL) recorded during resting-state EEG while seated. PD3 comprised 56 participants (28 PD, 28 CTL) who completed a reward-based feedback learning task. All datasets were recorded with 64-channel EEG systems following the international 10–20 montage. Sampling frequencies ranged from 250 Hz to 1000 Hz, and channel metadata were preserved in accordance with BIDS specifications. When provided, event markers and participant metadata were extracted from the corresponding participants.tsv files and events files within each dataset.

3.2 Preprocessing and Task Procedure

As shown in Figure 1-3, our methodology is structured into three primary stages: preprocessing, feature extraction, and model formulation. During preprocessing, raw EEG signals are cleaned to remove noise and physiological artifacts that may distort neural activity. The cleaned signals are then subjected to feature extraction, where the Fast Fourier Transform (FFT) is applied to convert time-domain signals into the frequency domain. Signal complexity is subsequently quantified using Shannon entropy. Finally, multiple classification models are trained on the extracted features, and the overall pipeline performance is evaluated using standard classification metrics.

EEG data preprocessing was carried out using both MNE-Python and EEGLAB, depending on dataset format. Signals were bandpass filtered between 1–40 Hz, with notch filtering at either 50 or 60 Hz to remove powerline interference. Independent Component Analysis (ICA) was applied to eliminate ocular and cardiac artifacts as shown in Figure 4.

Principal Component Analysis (PCA) was used to reduce dimensionality. Data were re-referenced to the average reference. For resting-state datasets, signals were segmented into 2-second epochs (as shown in Figure 5) while task-based datasets were segmented into trial-based epochs.

Noisy channels were interpolated, and epochs with amplitudes exceeding ±100 μV were excluded from further analysis. For each EEG epoch, a comprehensive feature set was extracted to capture time-domain, frequency-domain, via Fast Fourier.

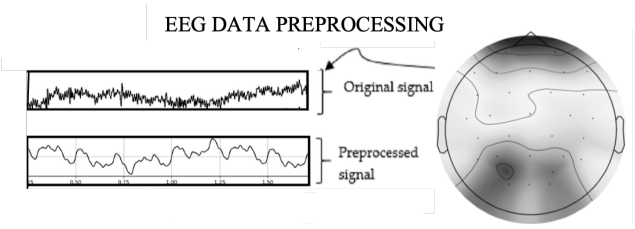

Figure 1: EEG preprocessing (Step 1): Raw scalp EEG signals (top) and corresponding preprocessed signals after filtering and artifact removal (bottom).

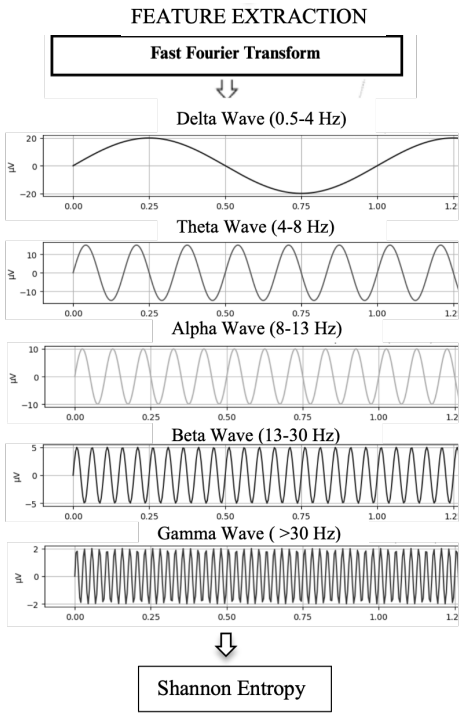

Figure 2: Feature Extraction (Step 2): Preprocessed EEG signals analyzed via FFT, with Shannon entropy applied to form feature vectors across channels.

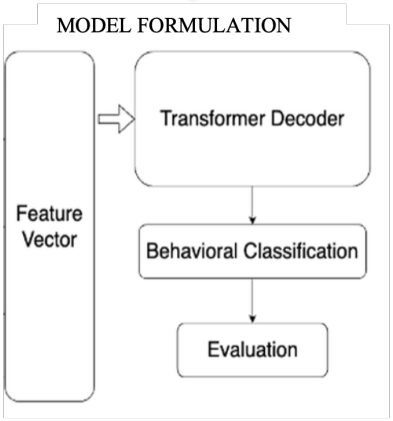

Figure 3: Model Formulation (Step 3): Feature vectors are processed by classical machine learning models or Transformer decoder for classification and evaluation.

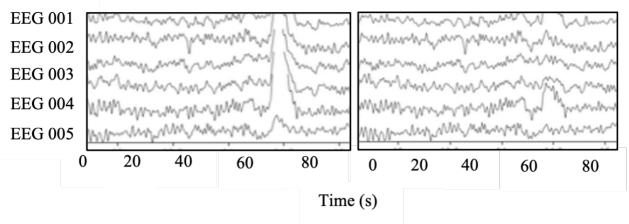

Figure 4: Raw EEG signal before (left) and cleaned signal after (right) preprocessing and the use of ICA-based artifact removal.

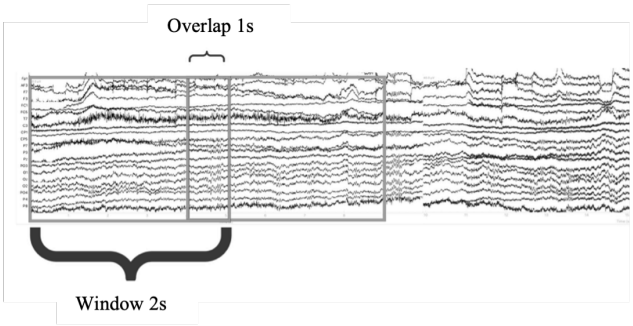

Figure 5: EEG preprocessing pipeline illustrating sliding-window epoch generation. Continuous EEG recordings are divided into 2-second epochs with a 1-second overlap, allowing adjacent windows to share temporal information while maintaining fixed-length input segments for downstream analysis.

3.3 Fast Fourier Transform (FFT)–Based Feature Extraction

To extract spectral characteristics from EEG signals, the Fast Fourier Transform (FFT) was applied to each preprocessed EEG epoch to convert time-domain signals into their frequency-domain representations. The discrete Fourier transform is defined by the Fourier matrix formulation in Equation (1), where the complex root of unity $\omega = e^{2\pi i/n}$ is given in Equation (2). Using this formulation, the time-domain EEG signal vector is mapped to its corresponding frequency-domain coefficients.The FFT algorithm exploits the structure of the Fourier matrix to reduce computational complexity by recursively decomposing the transformation into smaller subproblems, as shown in Equation (3). This divide-and-conquer strategy reduces the computational cost from $O(n^2)$ to $O(n\log n)$as illustrated in Equation (4). The resulting frequency-domain coefficients $\hat{f}_k$, computed according to Equation (5), represent the contribution of each frequency component in the EEG signal, while Equation (6) describes the inverse transformation back to the time domain. FFT-derived frequency coefficients were subsequently used to compute spectral features, including relative power within standard EEG frequency bands (delta, theta, alpha, beta, and gamma). These frequency-domain features provide compact representations of neural oscillatory activity and were incorporated into the feature vector used for Parkinson's disease classification. Spectral features were computed consistently across all models to ensure that performance differences reflect modeling capacity rather than feature discrepancies.

$$\begin{bmatrix} 1 & 1 & 1 & \cdots & 1 \\ 1 & \omega_n & \omega_n^2 & \cdots & \omega_n^{n-1} \\ 1 & \omega_n^2 & \omega_n^4 & \cdots & \omega_n^{2(n-1)} \\ \vdots & \vdots & \vdots & \ddots & \vdots \\ 1 & \omega_n^{n-1} & \omega_n^{2(n-1)} & \cdots & \omega_n^{(n-1)^2} \end{bmatrix} \begin{bmatrix} \widehat{f_0} \\ \widehat{f_1} \\ \widehat{f_2} \\ \vdots \\ \widehat{f_n} \end{bmatrix} = \begin{bmatrix} f_0 \\ f_1 \\ f_2 \\ \vdots \\ f_n \end{bmatrix} \quad (1)$$

$$\omega = e^{2\pi i/n} \quad (2)$$

$$F = F_n \hat{f} = \begin{bmatrix} I_{n/2} & D_{n/2} \\ I_{n/2} & D_{n/2} \end{bmatrix} \begin{bmatrix} F_{n/2} & 0 \\ 0 & F_{n/2} \end{bmatrix} \begin{bmatrix} \hat{f}even \\ \hat{f}odd \end{bmatrix} \quad (3)$$

$$O(n^2) \quad F_n \to F_{\frac{n}{2}} \to F_{\frac{n}{4}} \to F_{\frac{n}{6}} \cdots \to F_2 \quad O(n * \log(n)) \quad (4)$$

$$\hat{f}_k = \sum_{i=0}^{n-1} f_i e^{-i2\pi jk}/n \quad (5)$$

$$f_k = (\sum_{i=0}^{n-1} \hat{f}_i e^{i2\pi jk}/n) \quad (6)$$

3.4 Shannon Entropy

And complexity-related characteristics, such as Shannon entropy, were extracted to quantify the irregularity and information content of the EEG signals.

$$\mathrm{H} = -\sum_{i=1}^{n} P(x_i) \cdot log_b \mathrm{P}(x_i) \quad (7)$$

Where, H: Shannon Entropy (a single number value, $P(x_i)$ is the probability of the i-th state or value in the signal, n is the total number of states or bins, and b is the base logarithm (commonly 2 for bits). A Higher entropy (e.g., 3–4 bits): More dynamic brain activity (e.g., problem solving). A Lower entropy (e.g., < 1 bit): Reduced complexity, often observed in PD patients. Time-domain features included the mean, standard deviation, skewness, kurtosis, and Hjorth parameters. Frequency-domain features consisted of relative power across standard EEG bands: delta (0.5–4 Hz), theta (4–8 Hz), alpha (8–13 Hz), beta (13–30 Hz), and gamma (30–40 Hz). Entropy-based features such as spectral entropy and permutation entropy were also computed. For task-based datasets (PD2 and PD3), event-related potential (ERP) features were extracted, including the amplitudes and latencies of components such as N100/P300 (PD2) and feedback-related potentials (PD3).

3.5 Analytical Strategy

We compared the classification performance of classical machine learning models and a deep learning approach. The classical models included logistic regression (LR), support vector machines (SVM), random forests (RF), and decision trees (DT). For deep learning, we implemented a Transformer-based neural network capable of modeling temporal and spectral dependencies across multichannel EEG inputs. To ensure robust and unbiased evaluation, we employed

stratified 5-fold group cross-validation with grouping by subject, preventing any subject from appearing in both training and test folds. This validation strategy approximates deployment-relevant generalization more closely than random epoch-level splitting and reduces over-optimistic performance estimates. Hyperparameters for classical models were optimized using grid search, while the Transformer model was trained using the Adam optimizer with early stopping based on validation loss. Model performance was evaluated using multiple metrics: sensitivity *(8)*, precision *(9)*, confusion matrices, and ROC AUC scores. The F1-score (10) was emphasized to balance precision and recall in the presence of class imbalance, and ROC AUC was used to assess the models' discriminative performance across thresholds.

$$Sensitivity = \frac{TP}{TP+FN} \times 100\% \quad (8)$$

$$Precision = \frac{TP}{TP+FP} \times 100\% \quad (9)$$

In (8) and (9), TP denotes true positives, TN denotes true negatives, FP denotes false positives, and FN denotes false negatives.

F1-score,

$$F1 - score = 2 \times \frac{Precision\ x\ Sensitivity}{Precision + Sensitivity} \times 100\% \quad (10)$$

4 Results

Table 1 summarizes the F1-score performance of the Transformer model and four classical machine learning classifiers across the three EEG datasets (PD1–PD3). Overall, the Transformer model achieved the highest classification performance on PD1 and PD3, with F1-scores of 99.33% and 98.35%, respectively. These results indicate a strong ability of the Transformer architecture to capture discriminative EEG patterns in both resting-state and task-based datasets. On the PD1 dataset, the Transformer model outperformed all baseline methods, exceeding Random Forest by more than 2% and outperforming Support Vector Machine and Logistic Regression by larger margins. Similar performance trends were observed for PD3, where the Transformer achieved the highest F1-score compared to all classical classifiers. These near-ceiling results likely reflect the relative homogeneity of acquisition protocols and participant characteristics within these datasets. For the PD2 dataset, performance differences among models were less pronounced. While the Transformer achieved an F1-score of 88.36%, Random Forest slightly outperformed it with an F1-score of 91.76%. In contrast, Support Vector Machine and Logistic Regression exhibited substantially lower performance on PD2, with F1-scores below 30%. The reduced performance across models on PD2 highlights the impact of increased heterogeneity, including mixed task conditions, medication variability, and recording differences. While the Transformer did not outperform all baselines on PD2, it remained competitive with nonlinear ensemble methods and substantially exceeded linear classifiers. Figures 6-11 further illustrate classification performance through confusion matrices and ROC–AUC curves for each dataset. The confusion matrices show strong diagonal dominance for the Transformer model on PD1 and PD3, indicating high agreement between predicted and true labels. ROC–AUC curves demonstrate consistently high discriminative capability for the Transformer across datasets, with near-perfect separation observed on PD1 and PD3.

F1-Scores					
Dataset	Transformer	RF	DT	SVM	LR
PD1	99.33%	97.09%	83.45%	90.24%	88.1%
PD2	88.36%	91.76%	86.08%	27.94%	27.36%
PD3	98.35%	94.6%	90.22%	27.15%	26.45%

Table 1: Comparison of F1-scores (%) for the Transformer model and classical machine learning classifiers (Random Forest, Decision Tree, Support Vector Machine, and Logistic Regression) across the three EEG datasets (PD1–PD3).

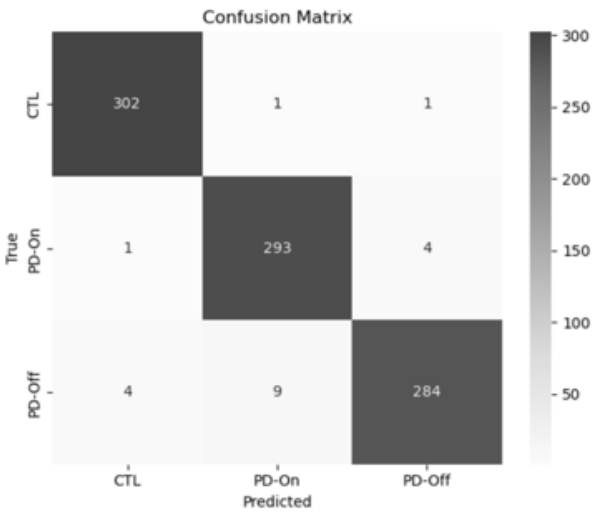

Figure 6: Confusion matrix for the Transformer model on the PD1 dataset, comparing true and predicted labels across the three categories: PD-ON, PD-OFF, and CTL. Strong performance is indicated by high values along the diagonal, reflecting accurate alignment between true and predicted classifications.

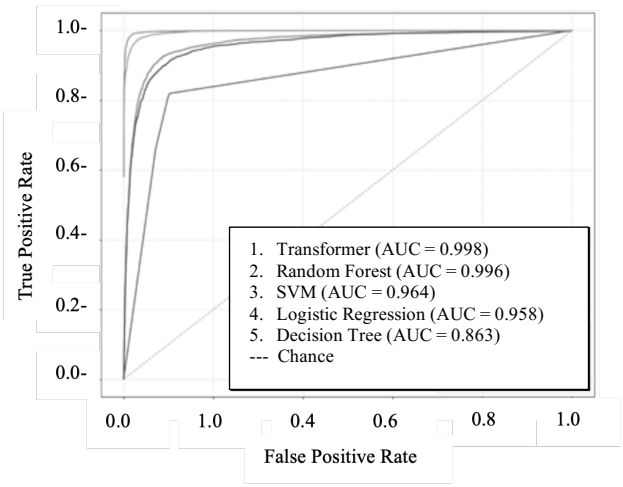

Figure 7: ROC–AUC curves (numbered from top left to bottom) for all classifiers evaluated on the PD1 dataset, including SVM, Transformer, Logistic Regression, Decision Tree, and Random Forest. The curves illustrate the trade-off between the true positive rate and false positive rate for each model.

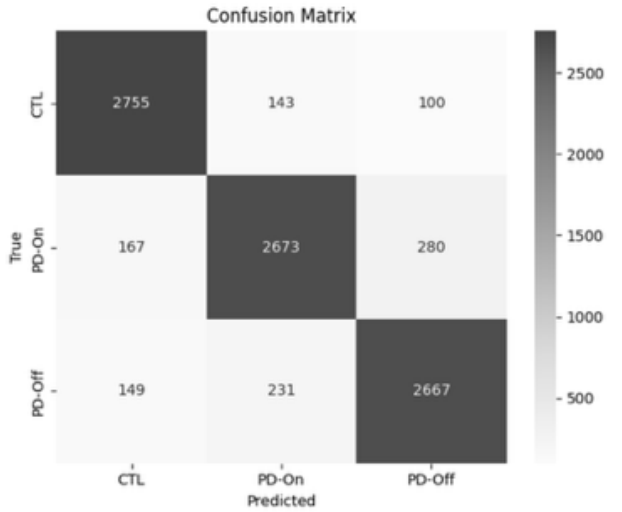

Figure 8: Confusion matrix for the Transformer model on the PD2 dataset, comparing true and predicted labels across the three categories: PD-ON, PD-OFF, and CTL. Strong performance is indicated by high values along the diagonal, reflecting accurate alignment between true and predicted classifications.

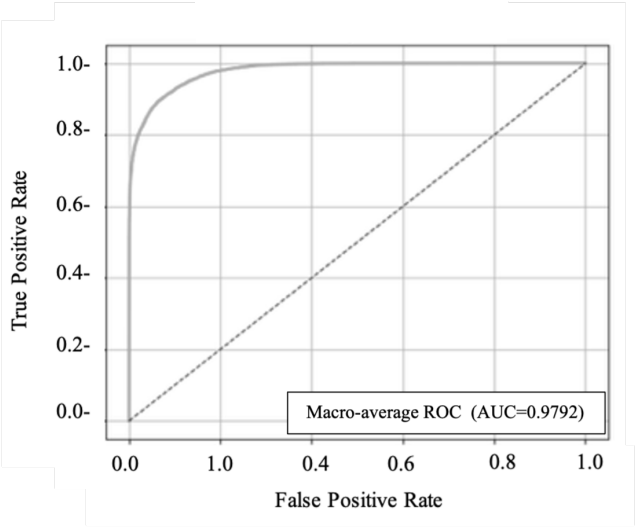

Figure 9: ROC–AUC curves (numbered from top left to bottom) for Transformer-Encoder deep learning classifier evaluated on the PD2 dataset. The curve illustrate the trade-off between the true positive rate and false positive rate for each model.

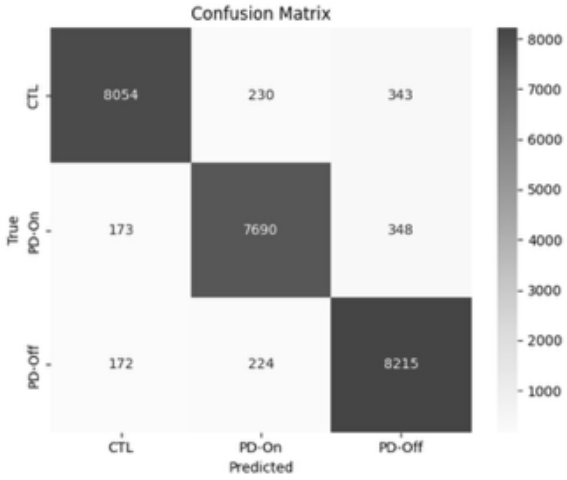

Figure 10: Confusion matrix for the Transformer model on the PD3 dataset, comparing true and predicted labels across the three categories: PD-ON, PD-OFF, and CTL. Strong performance is indicated by high values along the diagonal, reflecting accurate alignment between true and predicted classifications.

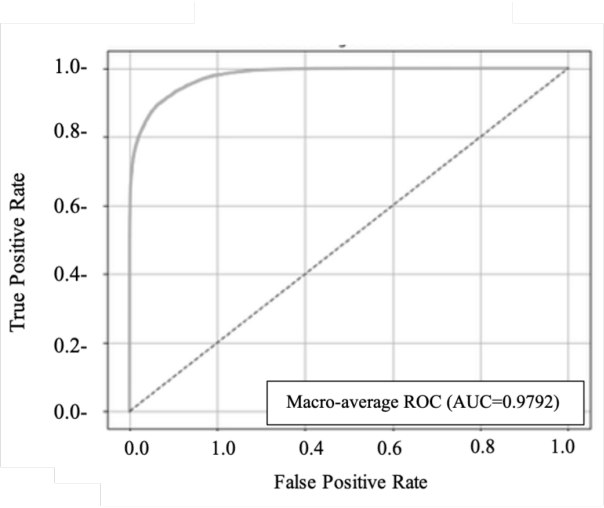

Figure 11: ROC–AUC (numbered from top left to bottom) curves for Transformer-Encoder deep learning classifier evaluated on the PD3 dataset. The curve illustrate the trade-off between the true positive rate and false positive rate for each model.

5 Discussion

Across the three datasets, the Transformer model demonstrated strong within-dataset performance, particularly on PD1 and PD3, indicating its capacity to model structured temporal and spectral EEG representations. These results suggest that the mechanism used by the model can effectively identify discriminative patterns when acquisition protocols and participant characteristics are relatively uniform. At the same time, the competitive performance of Random Forest across datasets highlights that handcrafted spectral and entropy features retain substantial discriminatory value. Because all models were trained on identical feature sets, performance differences reflect modeling capacity rather than feature differences.

The reduced performance observed on PD2 provides important context for interpreting the overall results. PD2 introduces greater heterogeneity, including variability in recording conditions, medication state, participant behavior, and task structure. Performance reduction across multiple models on this dataset underscores a well-documented challenge in EEG classification: sensitivity to non-stationarity and inter-site variability. PD2 serves as a realistic stress test of robustness under heterogeneous conditions. While the Transformer did not outperform all baselines on PD2, it remained competitive with ensemble methods and substantially exceeded simpler models, suggesting that temporal modeling provides advantages under increased complexity.

Although near-ceiling F1-scores were achieved on PD1 and PD3, these findings should be interpreted with caution. High classification metrics may be influenced by engineered feature representations, limited sample sizes, and relative dataset uniformity. To mitigate overfitting and optimistic bias, all evaluations employed subject-wise grouped cross-validation, ensuring that no participant contributed data to both training and testing sets. This validation strategy provides a realistic estimate of generalization, although cross-dataset transfer remains a challenge.

From a broader perspective, this study contributes to understanding how sequence models behave under noisy high-dimensional sensory data. EEG signals provide a controlled yet challenging testbed characterized by temporal dependency, signal noise, and acquisition variability. The findings illustrate both the promise and the limitations of temporal modeling in such environments. While the model can prioritize informative spectral and temporal patterns, robustness remains dependent on dataset structure and variability. Future work incorporating data harmonization and larger multi-site datasets will be necessary to strengthen generalization.

6 Conclusion

This study provides a systematic evaluation of a Transformer model for multi-class Parkinson's disease classification using structured EEG features across three heterogeneous datasets. The model achieved strong within-dataset performance on relatively uniform datasets PD1 and PD3 and competitive performance on a more heterogeneous dataset PD2, highlighting both the effectiveness and the limitations of temporal modeling under data variability.

The primary contribution of this work lies in rigorous multi-dataset benchmarking under subject-wise grouped cross-validation. By isolating modeling capacity from feature engineering and explicitly analyzing performance variation across datasets, the study clarifies how temporal modeling behaves under different levels of heterogeneity.

The results show that the model can effectively operate on physiologically interpretable spectral and entropy-based representations, supporting structured and explainable decision processes. At the same time, performance variability across datasets underscores the challenge of robustness to non-stationarity and inter-site differences in EEG classification.

Future work should focus on cross-dataset evaluation, data harmonization techniques, and expanded multi-site data collection to further assess generalizability. By examining temporal modeling under realistic sensory variability,

this study contributes to the broader goal of designing systems that are reliable, interpretable, and capable of accurate decision-making in complex and variable environments.

Acknowledgments

This material is based on work supported by the Department of the War (DOW) under the DOW No. FA955023D0001. Any opinions, findings, conclusions, or recommendations expressed in this material are those of the author(s) and do not necessarily reflect the views of the Department of the Air Force. The work was conducted in the Department of Biology and the Department of Mathematics and Computer Science at Tougaloo College, a member of the Research Institute for Tactical Autonomy (RITA) University Affiliated Research Center (UARC) led by Howard University.

This work was also funded in part by the NSF Implementation Grants # 1912191 (J. M)/2510537 (M.F), Research Initiation Award # 2300445 (X.W.), and HBCU-Targeted Infusion Project Award # 2205788 (M.F) at Tougaloo College. We deeply appreciate Dr. Kevin Schmidt, TPOC, from AFRL/RYZA, for his guidance and support in this project.

References

Betrouni, N.; Delval, A.; Chaton, L.; Defebvre, L.; Duits, A.; Moonen, A.; Leentjens, A. F. G.; and Dujardin, K. 2019. Electroencephalography-based machine learning for cognitive profiling in Parkinson's disease: Preliminary results. Movement Disorders 34(2): 210–217. https://doi.org/10.1002/mds.27528.

Brittain, J. S., and Brown, P. 2014. Oscillations and the basal ganglia: Motor control and beyond. NeuroImage 85(2): 637–647. https://doi.org/10.1016/j.neuroimage.2013.05.084.

Delorme, A.; Sejnowski, T.; and Makeig, S. 2007. Enhanced detection of artifacts in EEG data using higher-order statistics and independent component analysis. NeuroImage 34(4): 1443–1449. https://doi.org/10.1016/j.neuroimage.2006.11.004.

Geraedts, V. J.; Koch, M.; Contarino, M. F.; Middelkoop, H. A. M.; Wang, H.; van Hilten, J. J.; Bäck, T. H. W.; and Tannemaat, M. R. 2021. Machine learning for automated EEG-based biomarkers of cognitive impairment during deep brain stimulation screening in patients with Parkinson's disease. Clinical Neurophysiology 132(5): 1041–1048. https://doi.org/10.1016/j.clinph.2021.01.021.

He, H., and Wu, D. 2020. Transfer learning for brain–computer interfaces: A Euclidean space data alignment approach. IEEE Transactions on Biomedical Engineering 67(2): 399–410. https://doi.org/10.1109/TBME.2019.2913914.

Holt, A. B.; Kormann, E.; Gulberti, A.; Pötter-Nerger, M.; McNamara, C. G.; Cagnan, H.; Baaske, M. K.; Little, S.; Köppen, J. A.; Buhmann, C.; Westphal, M.; Gerloff, C.; Engel, A. K.; Brown, P.; Hamel, W.; Moll, C. K. E.; and Sharott, A. 2019. Phase-dependent suppression of beta oscillations in Parkinson's disease patients. Journal of Neuroscience 39(6): 1119–1134. https://doi.org/10.1523/JNEUROSCI.1913-18.2018.

Jung, T. P.; Makeig, S.; Westerfield, M.; Townsend, J.; Courchesne, E.; and Sejnowski, T. J. 2000. Removal of eye activity artifacts from visual event-related potentials in normal and clinical subjects. Clinical Neurophysiology 111(10): 1745–1758. https://doi.org/10.1016/S1388-2457(00)00386-2.

Kurbatskaya, A.; Jaramillo-Jimenez, A.; Ochoa-Gomez, J. F.; Bronnick, K.; and Fernandez-Quilez, A. 2023. Machine learning-based detection of Parkinson's disease from resting-state EEG: A multi-center study. In Proceedings of the Annual International Conference of the IEEE Engineering in Medicine and Biology Society, 1–4. https://doi.org/10.1109/EMBC40787.2023.10340700.

Little, S., and Brown, P. 2014. The functional role of beta oscillations in Parkinson's disease. Parkinsonism & Related Disorders 20(Suppl 1): S44–S48. https://doi.org/10.1016/S1353-8020(13)70013-0.

Subasi, A., and Gursoy, M. I. 2010. EEG signal classification using PCA, ICA, LDA and support vector machines. Expert Systems with Applications 37(12): 8659–8666. https://doi.org/10.1016/j.eswa.2010.06.065.

Tarakad, A., and Jankovic, J. 2017. Diagnosis and management of Parkinson's disease. Seminars in Neurology 37(2): 118–126. https://doi.org/10.1055/s-0037-1601888.

Tysnes, O. B., and Storstein, A. 2017. Epidemiology of Parkinson's disease. Journal of Neural Transmission 124(8): 901–905. https://doi.org/10.1007/s00702-017-1686-y.

Zhang, H.; Zhou, Q. Q.; Chen, H.; Hu, X. Q.; Li, W. G.; Bai, Y.; Han, J. X.; Wang, Y.; Liang, Z. H.; Chen, D.; Cong, F. Y.; Yan, J. Q.; and Li, X. L. 2023. The applied principles of EEG analysis methods in neuroscience and clinical neurology. Military Medical Research 10(1): 67. https://doi.org/10.1186/s40779-023-00502-7.